Electronic Supplementary Material (ESI) for Journal of Materials Chemistry A.

Supporting Information

Engineering One-Dimensional and Hierarchical PtFe Alloy Assemblies towards Durable Methanol Electrooxidation

*Lijuan Wang, Xinlong Tian, Yangyang Xu, Shahid Zaman, Kai Qi, Hongfang Liu and Bao Yu Xia**

Key Laboratory of Material Chemistry for Energy Conversion and Storage (Ministry of Education), Key Laboratory of Material Chemistry and Service Failure, School of Chemistry and Chemical Engineering, Wuhan National Laboratory for Optoelectronics, Huazhong University of Science and Technology (HUST), 1037 Luoyu Road, Wuhan 430074, P. R. China

**Corresponding authors: byxia@hust.edu.cn (B.Y. Xia)*

Experimental Section

1. Preparation

Platinum acetylacetonate, iron acetylacetonate were purchased from Shanghai Mackin Biochemical Co., Ltd. Oleylamine was from Aladdin. Hexadecyl trimethyl ammonium chloride and glucose were purchased from Shanghai Chemical Co., Ltd. PtRu/C and Pt/C (20 wt%, with the Vulcan XC-72R carbon) were from Johnson Matthey. All the chemical reagents were in analytical level and used as received.

In a typical synthesis of PtFe samples, platinum acetylacetonate ($Pt(acac)_2$, 20 mg), iron acetylacetonate ($Fe(acac)_2$, 4.3 mg), Hexadecyl trimethyl ammonium chloride (CTAC, 100 mg) and glucose (180 mg) were dissolved in oleylamine (OAm, 10 mL) with sonication for 2 h. Consequently, the mixture was heated to 180 °C from room temperature and held at 180 °C for 8 h in an oil bath. The obtained materials were washed and centrifuged three times with ethanol/cyclohexane mixture (volume 3/1). Then the obtained samples were dried naturally for further tests. The synthesis processes of Pt_7Fe, Pt_5Fe, $Pt_{3.5}Fe$ and Pt_3Fe are the same with Pt_4Fe except the addition amount of 1.6, 2.5, 3.3 and 6.6mg $Fe(acac)_2$, respectively.

2. Characterization

X-ray diffraction (XRD) patterns was conducted using a powder diffractometer (X'Pert-Pro) with a Cu radiation source (Cu Kα, λ=0.15406 nm) from 30 ^{o} to 90^{o} with a rate of 2^{o} min^{-1}. The size and morphology were studied by transmission electron microscopy (TEM) on TecnaiG2 20 (Philips) at an accelerating voltage of 200 kV equipped with an energy dispersive spectrometer (EDS) spectrum. High-angle annular dark field (HAADF) images and the corresponding energy dispersive spectrometer (EDS) elemental mapping were performed on scanning transmission electron microscopy (STEM) mode on an aberration-corrected FEI Titan

G2 60-300 field emission transmission electron microscope, operated at 300 kV (α_{max} = ~100 mrad).X-ray photoelectron spectroscopy (XPS) spectra were obtained on a monochromatic Al-Kα X-ray source (hv = 1486.6 eV, Thermo Scientific, ESCALAB 250 XI). The actual compositions were determined by evaluating the inductively coupled plasma mass spectrometer (ICP-MS, Perkin Elmer Elan-6000).

3. Electrochemical test

The catalysts were prepared by loading the synthesized samples on the commercial carbon support, and the Pt loading amount was set at 20 wt%. In brief, proper amount of PtFe sample (10.7 mg) and 40 mg carbon was mixed in cyclohexane under sonicating for 5 h, and then the resulting mixture was dried at an oven at 50 °C overnight. PtRu/C and Pt/C (Johnson Matthey, 20 wt%, with the Vulcan XC-72R carbon) were used for comparison. The electrochemical tests were all collected on Metrohm PGSTAT302N workstation. The glassy carbon electrode (GCE, 5 mm inner diameter, 0.196 cm^2) was adopted as the working electrode. A platinum wire and Ag/AgCl (KCl-saturated) electrode were used as the counter and reference electrode, respectively. the catalyst solution was made by sonicating the mixture of catalyst (2 mg), isopropanol (950 µL) and Nafion (5 wt%, 50 µL) for 30 min, and then 5 µL of the solution was spread onto the GCE and dried naturally for further electrochemical tests. The Pt loadings of all the samples were controlled by 10 µg cm^{-2}.

Cyclic voltammetry (CV) and MOR activity characterization of the catalysts were performed at a potential window from -0.2 to 1.0 V (vs. Ag/AgCl) in N_2-saturated 0.1 M $HClO_4$ solution and 0.1 M $HClO_4$ + 0.5 M CH_3OH solution, respectively, at a scanning rate of 50 mV s^{-1}. The electrochemical active area (ECSA) was derived from the CV by integrating the hydrogen under potential desorption charge. CV curves were normalized to Pt loadings and ECSA to obtain the mass and specific activity, respectively. The chronoamperometry curves were obtained by holding the electrode at a constant potential (0.5 V (vs. Ag/AgCl).) for 5000 s in N_2-saturated 0.1 M $HClO_4$ + 0.5 M CH_3OH solution, and accelerated durability test (ADT) were performed in N_2-saturated 0.1 M $HClO_4$ solution for lasting 10,000 cycles (0.4–0.8 V(vs. Ag/AgCl).). Electrochemical impedance spectroscopy (EIS) measurements were conducted to study the electron transfer rate of the catalysts. EIS signals were recorded in the frequency range of 10^5~10^{-1} Hz using a sine wave with an amplitude of ±10 mV, at an applied potential of 0.45 V (vs. Ag/AgCl).

The CO stripping curves of the samples were collected as follows: First, the working electrode was immersed into the CO-saturated 0.1 M $HClO_4$ solution, and in order to make sure that all the exposed Pt atoms were covered by CO, the CO gas flow (20 sccm) was bubbled to the solution for 30 minutes with the electrode was kept at -0.2 V (vs Ag/AgCl). Then the dissolved CO was driven away by bubbling N_2 flow (50 sccm) for 20 min, and the first forward current scan was recorded.

Figures

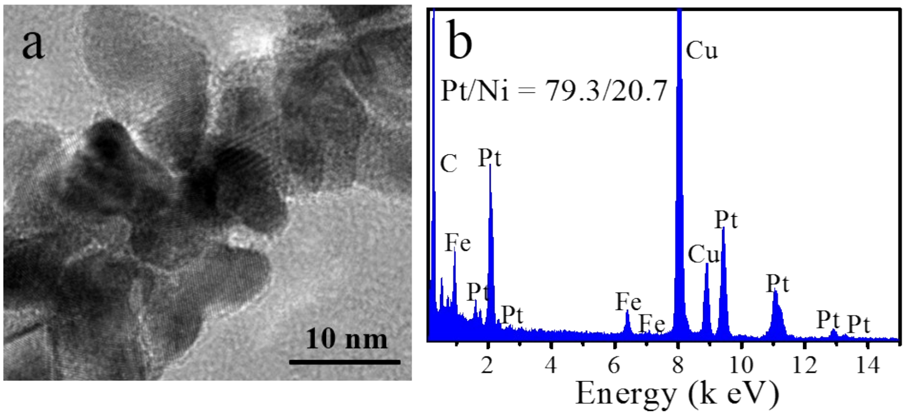

Figure S1. (a) TEM and the corresponding (b) EDS profile of synthesized PtFe samples.

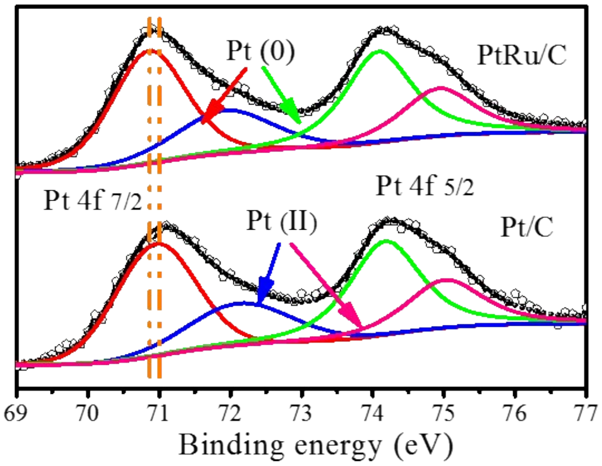

Figure S2. Pt 4f XPS spectrum of commercial PtRu/C and Pt/C catalysts.

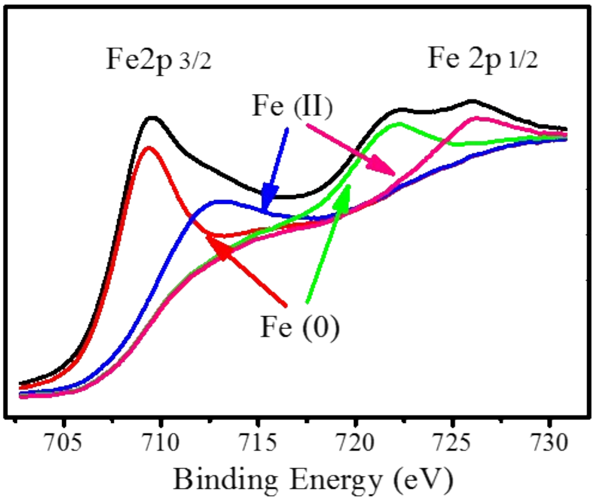

Figure S3. Fe 2p XPS spectrum of PtFe/C catalyst.

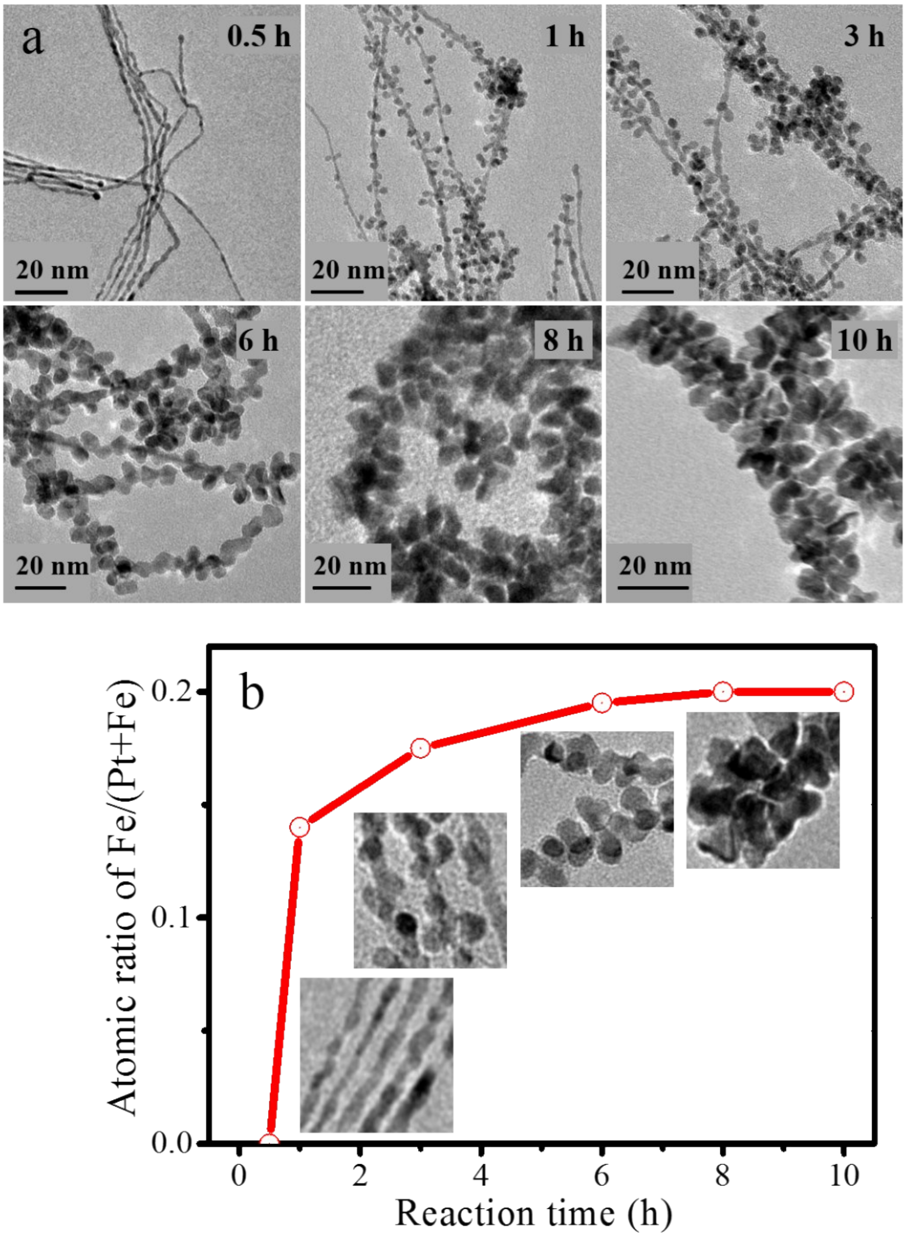

Figure S4. (a) TEM images of PtFe with various reaction times. (b) The atomic ratio of Fe in PtFe samples, and the corresponding TEM images with different reaction times.

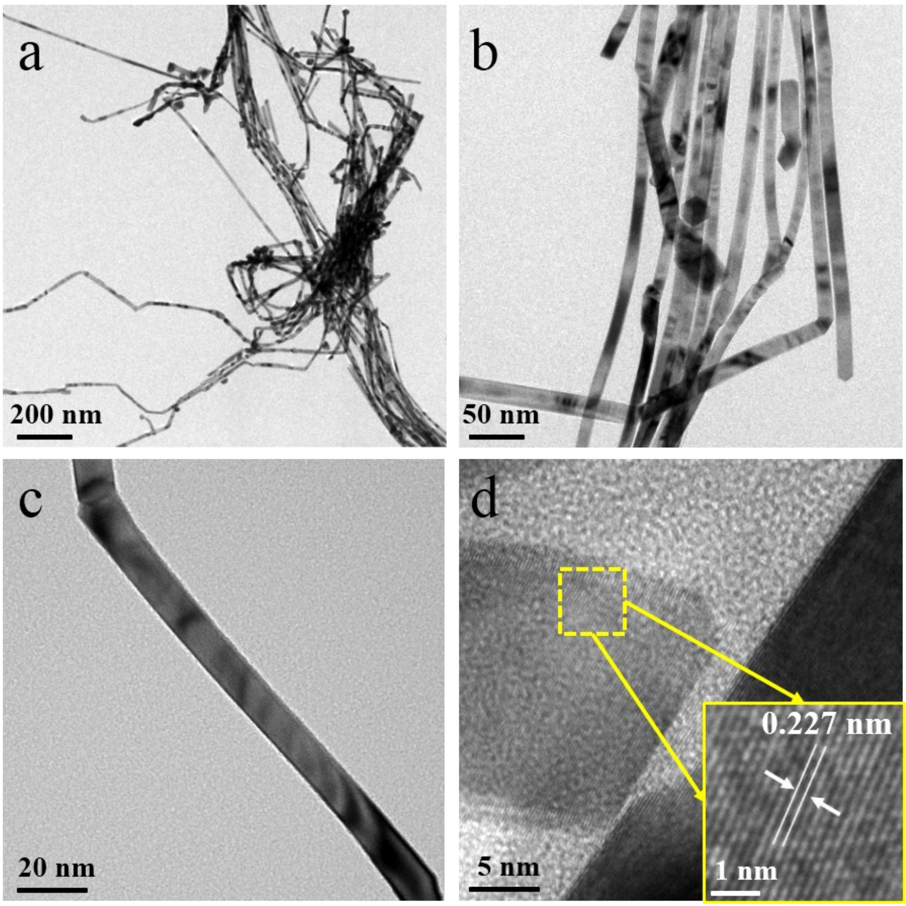

Figure S5. (a-d) TEM images of pure Pt nanowires.

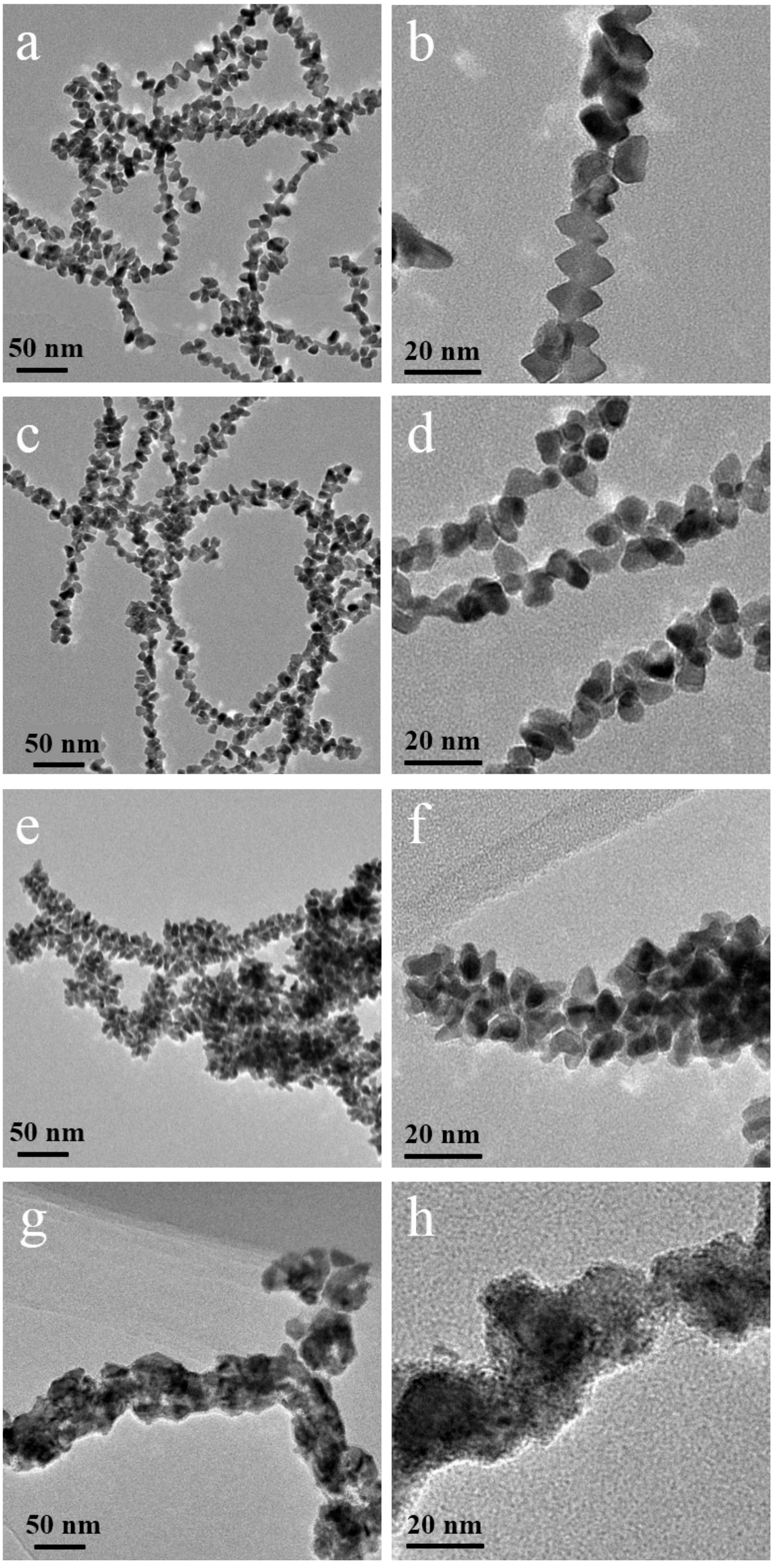

Figure S6. TEM images of (a,b) Pt_7Fe, (c,d) Pt_5Fe, (e,f) $Pt_{3.5}Fe$ and (g,h) Pt_3Fe samples.

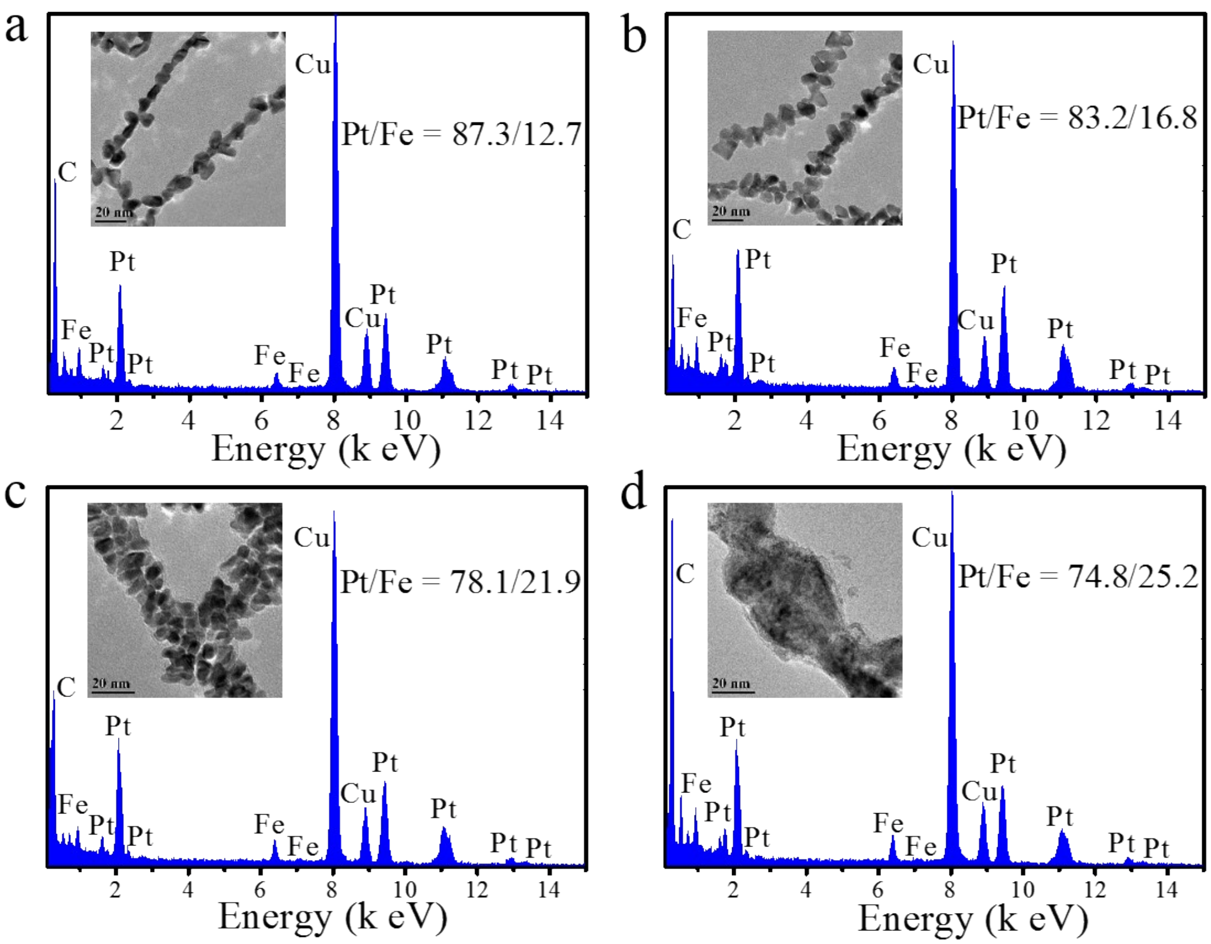

Figure S7. TEM-EDS profile of (a) Pt_7Fe, (b) Pt_5Fe, (c) $Pt_{3.5}Fe$ and (d) Pt_3Fe samples, and the insets is the corresponding TEM images.

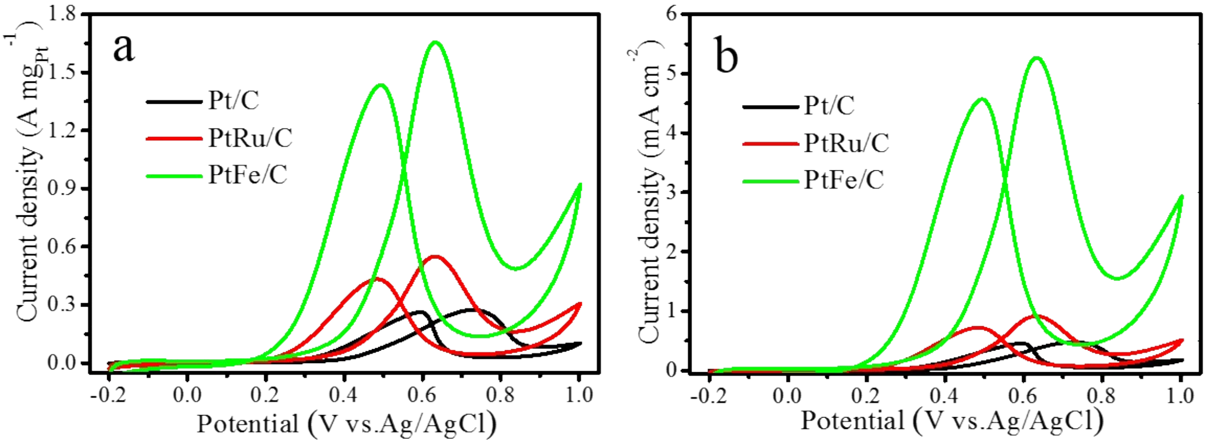

Figure S8. (a) Mass activities, (b) specific activities of Pt/C, PtRu/C and PtFe/C catalysts.

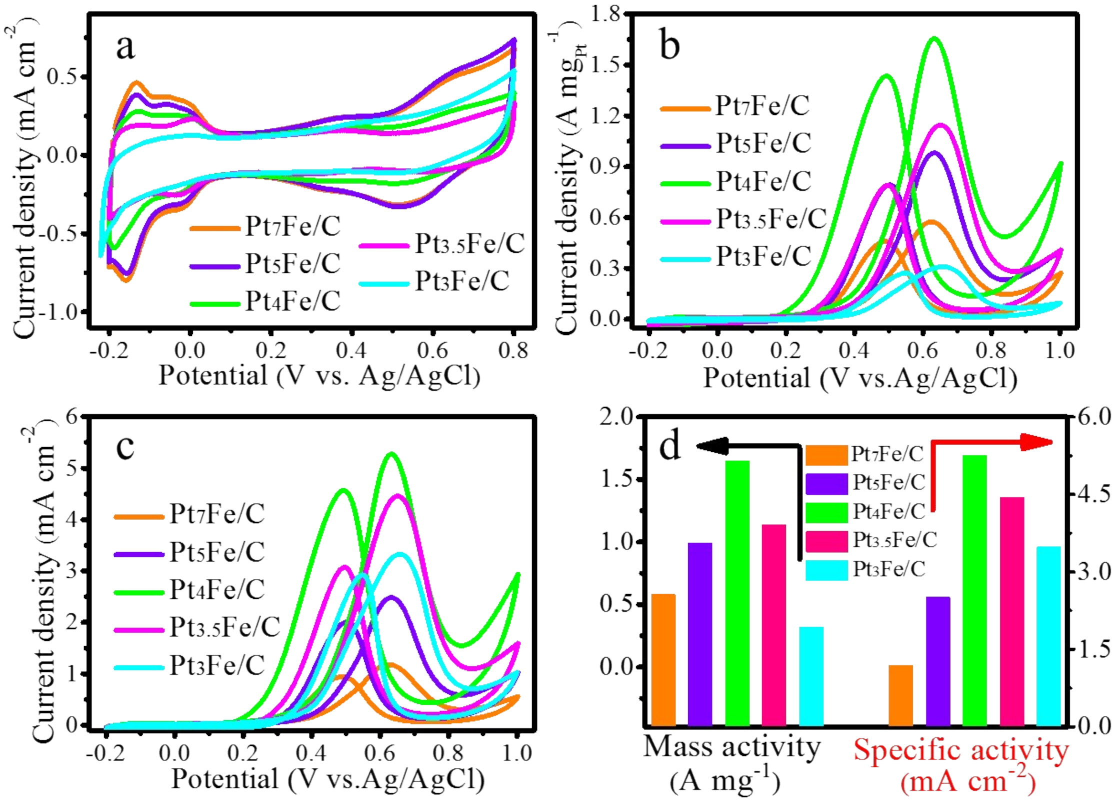

Figure S9. (a) CV in N_2-saturated 0.1 M $HClO_4$ solution. (b) Mass and (c) specific activities, and (d) the performance comparison of Pt_7Fe, Pt_5Fe, Pt_4Fe, $Pt_{3.5}Fe$ and Pt_3Fe in 0.1 M $HClO_4$ + 0.5 M CH_3OH solution.

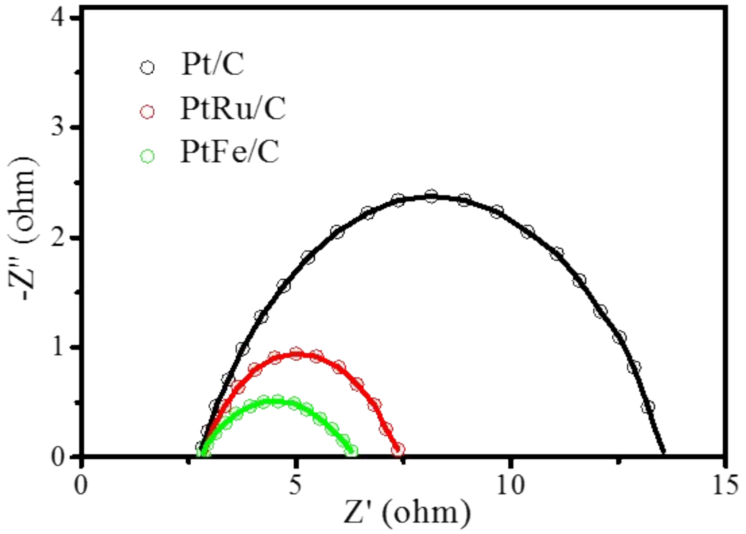

Figure S10. Nyquist plots of Pt/C, PtRu/C and PtFe/C catalysts obtained at 0.45 V (vs Ag/AgCl). in 0.1 M $HClO_4$ + 0.5 M CH_3OH solution.

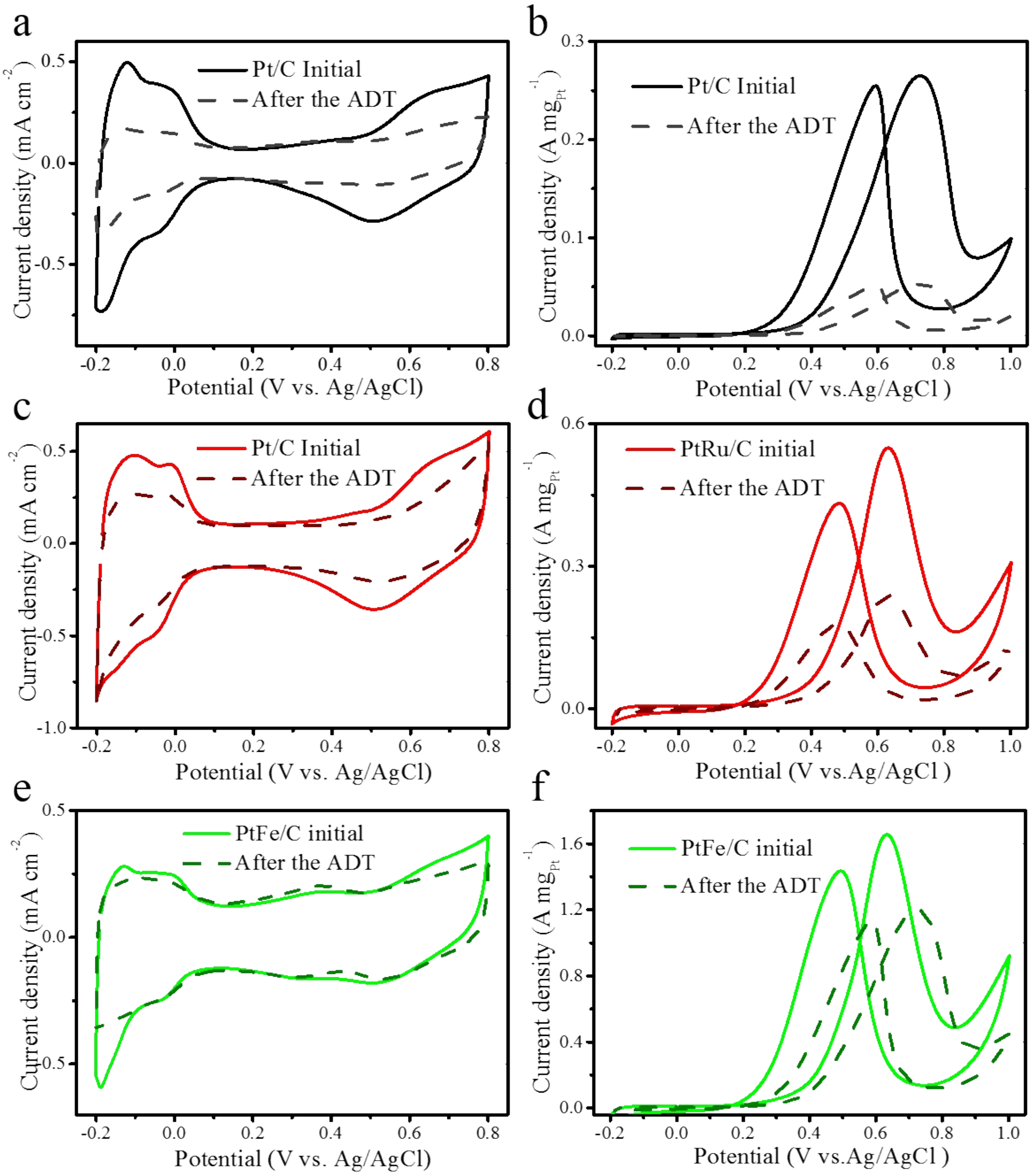

Figure S11. CV curves (a. c. e) and mass activity evolutions (b, d, f) of (a,b) Pt/C, (c,d) PtRu/C and (e,f) PtFe/C after the ADT.

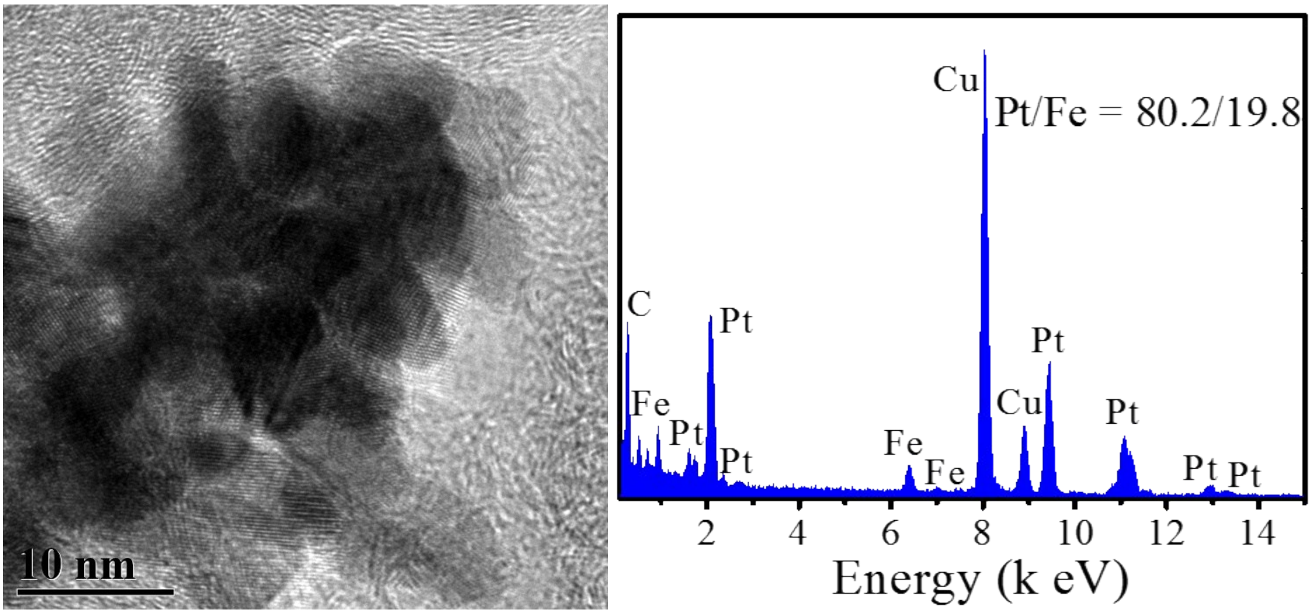

Figure S12. TEM image and EDS profile of PtFe samples after the ADT.

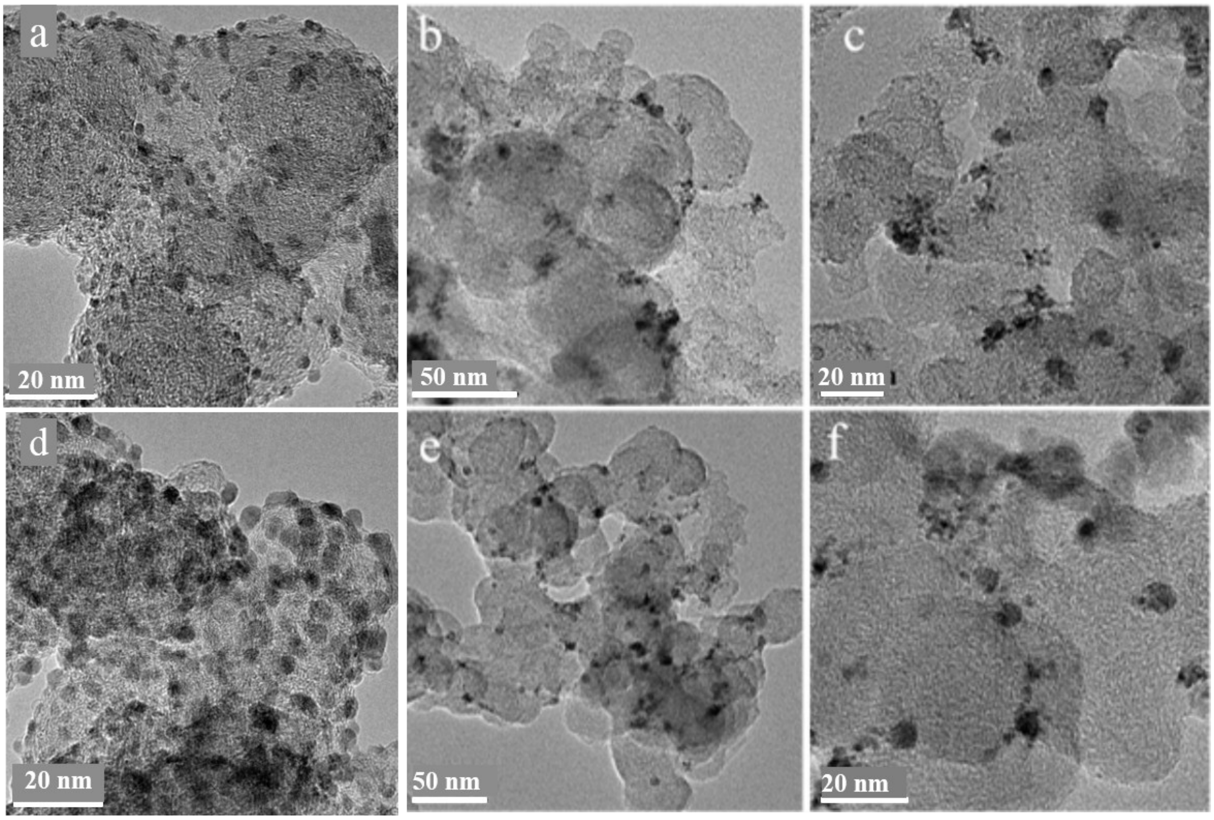

Figure S13TEM image of initial Pt/C (a) and after the ADT (b, c), TEM images of initial PtRu/C (d) and after the ADT (e, f).

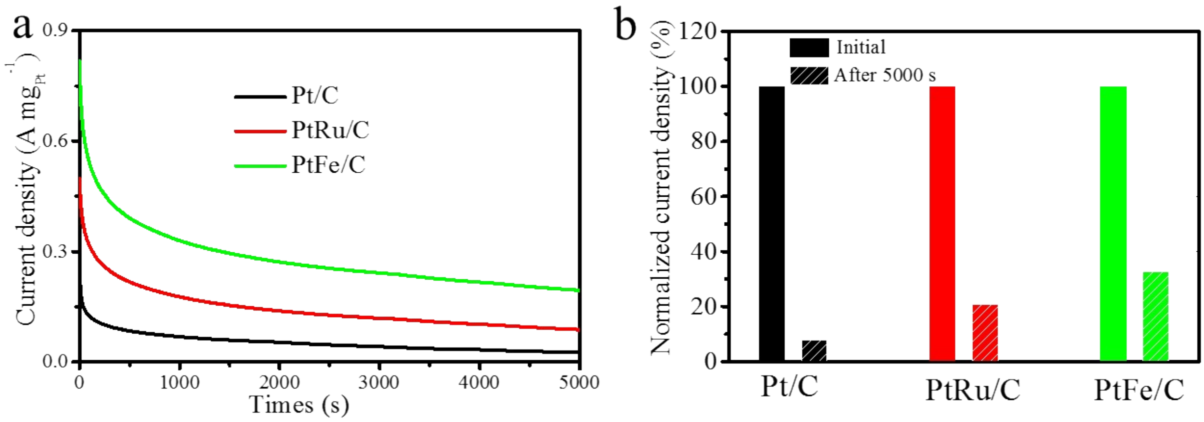

Figure S14. (a) Chronoamperometry curves of Pt/C, PtRu/C and PtFe/C in 0.1 M $HClO_4$ + 0.5 M CH_3OH solution, and the potential was held at 0.5 V (vs. Ag/AgCl). (b) The normalized current density corresponding to the current at 5000 s and the initial of the samples.

Table S1. The on-set potential, mass activity and specific activity of the catalysts recorded from Figure 3.

Catalyst	On-set potential (V)	Mass activity (A mg_{Pt}^{-1})	Specific activity (mA cm^{-2})
Pt/C	0.38	0.27	0.46
PtRu/C	0.28	0.56	1.01
PtFe/C	0.19	1.65	5.25

Table S2. Comparisons of the MOR performance for Pt-based catalysts in recently published papers.

Catalyst	Mass activity	Specific activity	ECSA	Durability		Reference
	$\text{A mg}_{\text{Pt}}^{-1}$	mA cm^{-2}	$\text{m}^2\ \text{g}^{-1}$	Cycles	Mass Activity retention/ %	
1D PtFe Alloy Assemblies	**1.65**	**5.26**	**31.4**	**1000**	**85.5%**	**This work**
				10000	**75.8%**	
Mesoporous Pt nanoparticles	0.405	1.29	32	/	/	Angew. Chem. Int. Ed., **2016**, 55,10037.
Pt NW/N-LDG	1.28	2.1	60.9	/	/	Small **2017**, 13, 1603013.
Pt nanosheets	~0.27	/	47.37	5000	73.6%	Adv. Mater.**2015**, 27,4430.
Mesoporous Pt nanosphere	0.2036	1.24	16.34	/	/	Angew. Chem. Int. Ed., **2015**, 54,11073.
PtZn nanoparticles	0.612	1.08	/	1000	96.8%	J. Am. Chem. Soc., **2017**, 139, 4762.
FePt nanoparticles	1.435	4.00	35.35	/	/	Nano Res., **2017**, 10, 2866.
AuPt nanoparticles /C	2.25	7.87	28.6	500	95.4%	J. Mater. Chem. A, **2018**,6, 104.
Atomic-Layer Pt on Intermetallic Pt_3Ga	1.094	7.195	/	1000	/	J. Am. Chem. Soc., **2018**, 140, 2773.
Pt–Co nanowires	0.471	/	45.2	1000	82%	Angew. Chem. Int. Ed., **2015**, 54, 3797.
$Ru@Pt_{0.5}/C$	1.3138	/	/	1000	84.1%	Nano Energy., 2016, 21, 247.
PtNi nanocrystals	0.696	1.37	51	/	/	Adv. Funct. Mater., **2018**, 28, 1704774.
PtRu nanowires	0.82	1.16	70.6	800	63.7%	J. Am. Chem. Soc., **2018**, 140, 1142.
porous $Pt_{72}Ru_{28}$ nanoalloys	1.70	10.98	15.5	4000	~50%	Adv. Energy Mater., **2017**, 7, 1601593.
PtCu nanowires	1.56	3.31	46.9	1000	72.9%	Nano Lett., **2016**, 16, 5037.
PtCu nanotubes	2.25	6.09	38	/	/	Energy Environ. Sci., **2017**, 10, 1751.
PtPb nanowires	1.21	2.41	50.5	1000	58.4%	Chem. Mater. **2016**,

						28, 4447.
AgAu@Pt nanoframes	0.48	1.96	24.6	/	/	Nanoscale, **2018**, 10, 2231.
PtCuCo nanoframes	4.11	13.3	30.9	1000	63.5%	Adv. Funct. Mater., **2018**, 28, 1706440.
PtBi@Pt nanoplate	1.1	3.18	33.9	/	/	ACS Catal., **2018**, 8, 5581.
PtPdRuTe nanotubes	1.26	2.96	42.6	1000	97.2%	J. Am. Chem. Soc., **2017**, 139, 5890.
Pd@PtNi nanoplates	0.782	0.957	42.40	/	/	Nano Lett., **2016**, 16, 7999.
Pt/CeO_2/PANI hollow nanorod	0.361	/	43.26	1000	97.9%	ACS Catal. **2016**, 6, 5198.